ELECTRONIC PROPERTIES
OF SOLID

Effect of Crystal Field on the Electronic Structure of the Two-Band Hubbard Model with Spin Crossover

Yu. S. Orlov[a,b,*], S. V. Nikolaev[a,b], and V. A. Dudnikov[a]

[a] *Kirensky Institute of Physics, Federal Research Center Krasnoyarsk Scientific Center, Siberian Branch, Russian Academy of Sciences, Krasnoyarsk, 660036 Russia*

[b] *Siberian Federal University, Krasnoyarsk, 660041 Russia*

*e-mail: jso.krasn@mail.ru

Abstract—We consider the change in the electronic structure of the two-band Hubbard model in the regime of strong electron correlations with spin crossover upon the passage through the crossover point depending on the crystal field growth. An abrupt semimetal–insulator–semimetal transition is detected during the passage through the spin crossover point in the absence of the spin–orbit interaction, which is accompanied by a jumpwise redistribution of the partial spectral weight between the poles of the Green function of Fermi quasiparticles. The role of the spin–orbit interaction and the change in the surface topology of surface of one-particle Green function zeros are considered.

1. INTRODUCTION

Spin crossover is a transition between the low-spin (LS) and high-spin (HS) states of the central ion of a transition $3d$ metal, which is observed in various coordination compounds under the action of external physical factors such as temperature, radiation, pressure, magnetic or electric field, or chemical factors (salvation, isomerization, ligand exchange reaction, and bond rupture) [1–3].

A theoretical description of spin crossovers is traditionally based on the single-ion pattern in which the HS state is stabilized by the intratomic Hund exchange interaction, while the LS state is stabilized by the crystal field that increases with the external pressure. For this reason, the ground HS state typical of an isolated ion changes to the LS state when the crystal field energy becomes equal to the energy of the Hund exchange interaction. In such a situation, spin crossover at zero temperature is a quantum phase transition in pressure with a topological order parameter determined by the Berry geometrical phase that changes abruptly by 2π at the transition point [4]; therefore, it would be interesting to investigate the band structure during spin crossover. This study is aimed at analysis of the evolution of the electronic band structure during the spin crossover based on the two-band Hubbard model considered for a 2D square lattice. In this case, the inclusion of multiparticle effects (Coulomb interaction of electrons) is of fundamental importance; for this reason, we are using here the formalism of Green's functions and the representation of Hubbard X operators.

2. MINIMAL MODEL

The minimal model of strongly correlated systems with spin crossover is the two-band Hubbard model that is widely used in theoretical analysis of the electronic, magnetic, and crystalline structure and the interrelation between different systems in the regime of strong and weak electron correlations [5–10]. The Hamiltonian of the model can be written in the form

$$H = H_t + H_{\text{Coulomb}}. \tag{1}$$

The first term

$$
\begin{aligned}
H_t &= \varepsilon_1 \sum_{i,\sigma} a^{\dagger}_{i,1,\sigma} a_{i,1,\sigma} + \varepsilon_2 \sum_{i,\sigma} a^{\dagger}_{i,2,\sigma} a_{i,2,\sigma} \\
&+ t_{11} \sum_{\langle i,j \rangle, \sigma} a^{\dagger}_{i,1,\sigma} a_{j,1,\sigma} + t_{22} \sum_{\langle i,j \rangle, \sigma} a^{\dagger}_{i,2,\sigma} a_{j,2,\sigma} \\
&+ t_{12} \sum_{\langle i,j \rangle, \sigma} (a^{\dagger}_{i,2,\sigma} a_{j,1,\sigma} + a^{\dagger}_{i,1,\sigma} a_{j,2,\sigma})
\end{aligned}
$$

includes the hopping of electrons between the nearest neighboring crystal lattice sites with energy levels ε_1 and $\varepsilon_2 = \varepsilon_1 + \Delta$, where Δ is the electron energy in the
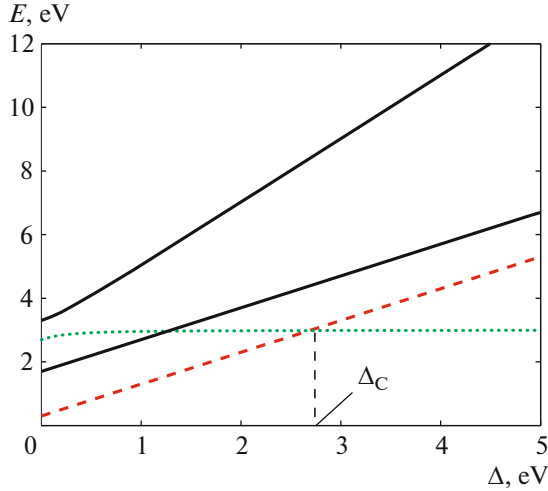
Fig. 1. (Color online) Dependence of the energy of terms on crystal field Δ. Red dashed line shows the position of the HS state ($S = 1$); green dotted curve indicates the position of the LS state ($S = 0$). Solid black lines are excited singlet states; Δ_C is the crossover point. Calculations were made for the following set of parameters: $U = 3$ eV, $V = 1$ eV, $J = 0.7$ eV, and $J' = 0.3$ eV.

crystal field and $t_{\lambda\lambda'}$ are the hopping integrals ($\lambda, \lambda' = 1, 2$). The second term

$$H_{\text{Coulomb}} = U \sum_{i,\lambda} a^{\dagger}_{i\lambda\uparrow} a^{\dagger}_{i\lambda\downarrow} a_{i\lambda\uparrow} a_{i\lambda\downarrow}$$

$$+ V \sum_{i,\lambda\neq\lambda'} a^{\dagger}_{i\lambda\uparrow} a^{\dagger}_{i\lambda'\downarrow} a_{i\lambda\uparrow} a_{i\lambda'\downarrow}$$

$$+ V \sum_{i,\lambda>\lambda',\sigma} a^{\dagger}_{i\lambda\sigma} a^{\dagger}_{i\lambda'\sigma} a_{i\lambda\sigma} a_{i\lambda'\sigma}$$

$$+ J \sum_{i,\lambda>\lambda',\sigma} a^{\dagger}_{i\lambda\sigma} a^{\dagger}_{i\lambda'\sigma} a_{i\lambda'\sigma} a_{i\lambda\sigma}$$

$$+ J \sum_{i,\lambda\neq\lambda'} a^{\dagger}_{i\lambda\uparrow} a^{\dagger}_{i\lambda'\downarrow} a_{i\lambda'\uparrow} a_{i\lambda\downarrow} + J' \sum_{i,\lambda\neq\lambda'} a^{\dagger}_{i\lambda\uparrow} a^{\dagger}_{i\lambda\downarrow} a_{i\lambda'\uparrow} a_{i\lambda'\downarrow}$$

contains the energy of the Coulomb interaction of electrons (the electron−electron interaction is considered in the Kanamori approximation [11]).

Apart from its relative simplicity, an important feature of such a two-orbital model is the possibility of formation of various localized multielectron (two-particle) states (terms) characterized by spin values $S = 0$, 1 (Fig. 1) and crossover between them in the case of half-filling ($N_e = 2$ is the number of electrons per crystal lattice site) and in the zeroth approximation in intersite jumps.

For example, for $N_e = 2$ and $t_{\lambda\lambda'} = 0$, Hamiltonian (1) has six eigenstates. In the region $\Delta < \Delta_C$, the ground state is the triplet ($S = 1$) HS state $|m_S\rangle$ with energy

$$E_{\text{HS}} = 2\varepsilon_1 + \Delta + V - J$$

(see Fig. 1, red dashed line), which is triply degenerate in spin projection $m_S = 0, \pm 1$:

$$|m_S\rangle = \begin{cases} a^{\dagger}_{1\uparrow} a^{\dagger}_{2\uparrow}|0\rangle, & m_S = +1, \\ \frac{1}{\sqrt{2}}(a^{\dagger}_{1\uparrow} a^{\dagger}_{2\downarrow}|0\rangle + a^{\dagger}_{1\downarrow} a^{\dagger}_{2\uparrow}|0\rangle), & m_S = 0, \\ a^{\dagger}_{1\downarrow} a^{\dagger}_{2\downarrow}|0\rangle, & m_S = -1, \end{cases}$$

while, for $\Delta > \Delta_C$, the ground state is the singlet ($S = 0$) LS state

$$|S\rangle = S_1(\Delta) a^{\dagger}_{1\uparrow} a^{\dagger}_{1\downarrow}|0\rangle - \sqrt{1 - C_1^2(\Delta)} a^{\dagger}_{2\uparrow} a^{\dagger}_{2\downarrow}|0\rangle$$

with energy

$$E_{\text{LS}} = 2\varepsilon_1 + (\Delta + U) - \sqrt{\Delta^2 - J'^2}$$

(see Fig. 1, green dotted curve). At the crossover point

$$\Delta = \Delta_C = \sqrt{(U - V + J)^2 - J'^2}$$

the energy levels of these states intersect. The remaining two states are excited singlet states

$$|S_1\rangle = \frac{1}{\sqrt{2}}(a^{\dagger}_{1\uparrow} a^{\dagger}_{2\downarrow}|0\rangle - a^{\dagger}_{1\downarrow} a^{\dagger}_{2\uparrow}|0\rangle),$$

$$|S_2\rangle = \sqrt{1 - C_1^2(\Delta)} a^{\dagger}_{1\uparrow} a^{\dagger}_{1\downarrow}|0\rangle + C_1(\Delta) a^{\dagger}_{2\uparrow} a^{\dagger}_{2\downarrow}|0\rangle$$

with energies

$$E_{S_1} = 2\varepsilon_1 + \Delta + V + J,$$

$$E_{S_2} = 2\varepsilon_1 + (\Delta + U) + \sqrt{\Delta^2 - J'^2},$$

respectively, where

$$C_1 = J' / \sqrt{J'^2 - (2\varepsilon_1 + U - E_{LS})^2}$$

is the normalization factor depending on Δ (in Fig. 1, these states are shown by the solid black line).

3. VARIATION OF THE ELECTRONIC STRUCTURE UPON AN INCREASE IN THE CRYSTAL FIELD

It is convenient to determine the electron spectrum of Hamiltonian (1) using Hubbard X operators $X^{pq} = |p\rangle\langle q|$ constructed for the eigenstates of Hamiltonian (1) in the absence of electron jumps (for $t_{\lambda\lambda'} = 0$) with different numbers of electrons $N_e = 1, 2, 3$ per crystal lattice site. Since the Hubbard operators form a linearly independent basis, any local operator can be

expressed in terms of a linear combination of X operators, including the one-electron annihilation (creation) operator at site i with orbital index λ and spin projection $\sigma = \pm 1/2$:

$$a_{i\lambda\sigma} = \sum_{p,q} |p\rangle\langle p|a_{i\lambda\sigma}|q\rangle\langle q| = \sum_{p,q} \gamma_{\lambda\sigma}(pq)X_i^{pq}. \qquad (2)$$

Alternately, since the number of different root vectors (pq) is finite, we can number them and juxtapose each vector to its number m; in this case,

$$a_{i\lambda\sigma} = \sum_{m} \gamma_{\lambda\sigma}(m)X_i^m \left(a_{a\lambda\sigma}^\dagger = \sum_{m} \gamma_{\lambda\sigma}^*(m)X_i^{\dagger m}\right).$$

In the representation of Hubbard X operators, Hamiltonian (1) has form

$$H = \sum_{i,p} E_p X_i^{pp} + \sum_{\langle i,j\rangle} \sum_{mn} t_{mn} X_i^{\dagger m} X_j^n.$$

Here, E_p is the energy of multielectron terms and

$$t_{mn} = \sum_{\sigma,\lambda,\lambda'} t_{\lambda\lambda'} \gamma_{\lambda\sigma}^*(m)\gamma_{\lambda'\sigma}(n)$$

is the renormalized hopping integral.

For deriving the dispersion relations for quasiparticle excitations, we will use the method of the equations of motion for the matrix Green function

$$D_{mn}(k,\omega) = \langle\langle X_k^m | X_k^{\dagger n}\rangle\rangle_\omega,$$

which are connected with one-electron Green function

$$G_{\lambda\sigma}(k,\omega) = \langle\langle a_{k\lambda\sigma} | a_{k\lambda\sigma}^\dagger\rangle\rangle_\omega$$

by relation

$$G_{\lambda\sigma}(k,\omega) = \sum_{m,n} \gamma_{\lambda\sigma}(m)\gamma_{\lambda\sigma}^*(n)D_{mn}(k,\omega).$$

In terms of the Fermi one-particle Green function, we can express the spectral density of one-particle excitations,

$$A_{\lambda\sigma}(k,\omega) = -\frac{1}{\pi}\operatorname{Im} G_{\lambda\sigma}(k,\omega+i\delta)$$

$$= -\frac{1}{\pi}\operatorname{Im}\sum_{m,n} \gamma_{\lambda\sigma}(m)\gamma_{\lambda\sigma}^*(n)D_{mn}(k,\omega+i\delta), \quad \delta \to +0$$

and the density of one-particle states for the given spin projection (N is the normalization factor),

$$N_{\lambda\sigma}(\omega) = \frac{1}{N}\sum_{k} A_{\lambda\sigma}(k,\omega)$$

In the Hubbard-I approximation for Green function $\hat{D}(k,\omega)$, we can write the following equation:

$$\hat{D}(k,\omega) = \hat{D}_0(\omega) + \hat{D}_0(\omega)\hat{t}(k)\hat{D}(k,\omega). \qquad (3)$$

Here,

$$D_0^{mn}(\omega) = \delta_{mn}F_m/(\omega - \Omega_m),$$

where

$$\Omega_m \equiv \Omega(pq) = E_p - E_q,$$

$F_m \equiv F(\mathrm{pq}) = \langle X^{pp}\rangle + \langle X^{qq}\rangle$ is the filling factor, which is referred to as the end factor in the diagram technique for the X operators [12]:

$$t_{mn}(k) = \sum_{\sigma,\lambda,\lambda'} \gamma_{\lambda\sigma}^*(m)\gamma_{\lambda'\sigma}(n)t_{\lambda\lambda'}(k),$$

where $t_{\lambda\lambda'}(k)$ is the Fourier transform of the hopping integrals. Solution (3) has the standard form for the mean field theory: $\hat{D}^{-1}(k,\omega) = \hat{D}_0^{-1}(\omega) - \hat{t}(k)$.

The dispersion relation for Fermi quasiparticles is determined by the equation for the pole of the matrix Green function $D_{mn}(k,\omega) = [(\hat{D}_0^{-1}(\omega) - \hat{t}(k))^{-1}]_{mn}$:

$$\det\|\delta_{mn}(\omega - \Omega_m)/F_m - t_{mn}(k)\| = 0.$$

This equation is close in form to the dispersion equation of the tight binding method in the one-electron band theory, but differs from it in the following two features: first, indices m and n label not one-electron orbitals, but one-particle excitations in a multielectron systems; second, the effective hopping integral is determined by product $t_{mn}(k)$ and filling factor F_m depending on the filling numbers of the initial and final states.

It should be noted that the following sum rule follows from exact representation (2) and the commutation relations for the Fermi operators:

$$\langle[a_{i,\lambda,\sigma}, a_{i,\lambda,\sigma}^\dagger]_+\rangle = 1 = \sum_{m} |\gamma_{\lambda\sigma}(m)|^2 F(m).$$

The consequence of this sum rule is the conservation of the total spectral weight in each band λ for any wavevector k:

$$\sum_{\sigma}\int A_{\lambda\sigma}(k,\omega)d\omega = 2.$$

In the diagram technique of the X operators, we can write the following Dyson equation for Green function $\hat{D}(k,\omega)$ [13]:

$$\hat{D}(k,\omega)$$
$$= [\hat{G}_0^{-1}(\omega) - \hat{P}(k,\omega)\hat{t}(k) + \hat{\Sigma}(k,\omega)]^{-1}\hat{P}(k,\omega). \qquad (4)$$

Here, $\hat{\Sigma}(k,\omega)$ and $\hat{P}(k,\omega)$ are the mass and force operators, respectively, and

$$G_{0mn}(\omega) = \delta_{mn}\frac{1}{\omega - \Omega_m}.$$

In the Hubbard-I approximation, the structure of exact Green function (4) is preserved, but the mass operator is set at zero, while force operator $P_{mn}(k,\omega) \to \delta_{mn}F_m$.
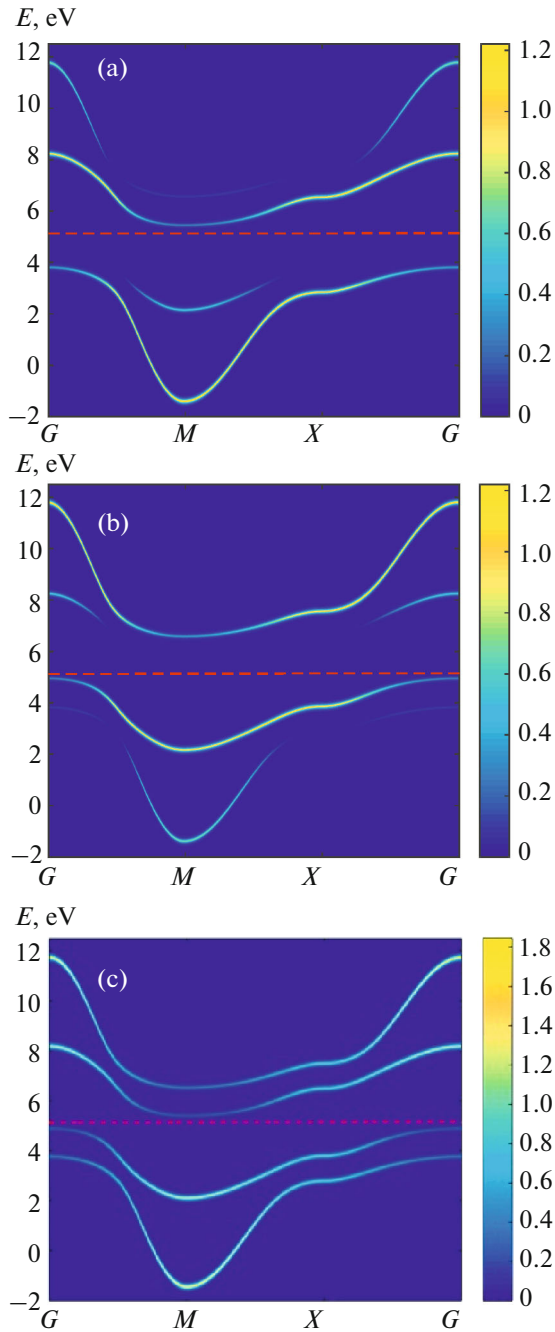
Fig. 2. (Color online) Dispersion of Fermi quasiparticle excitations calculated for the HS phase at $\Delta = 1$ eV. Red dashed horizontal line shows the position of the Fermi level in the bandgap. Colored curves show the distribution of partial spectral weight of quasiparticle excitations in the first Brillouin zone for (a) $\lambda = 1$ (ε_1), (b) $\lambda = 2$ (ε_2), and (c) spectral weight.

Fig. 3. (Color online) Dispersion of Fermi quasiparticle excitations calculated for the HS phase at $\Delta = 1.64$ eV. Dielectric gap $E_g = 0$ eV; the Fermi surface of the electron and hole types opens at points $G(0, 0)$, $M(1, 1)$, respectively, of the first Brillouin zone. Colored curves show the distribution of partial spectral weight of quasiparticle excitations in the first Brillouin zone for (a) $\lambda = 1$ (ε_1), (b) $\lambda = 2$ (ε_2), and (c) total spectral weight.

Figures 2–7 illustrate the variation of the electron spectrum and the Fermi surfaces depending on the increase of crystal field Δ. All calculations were performed at $T = 0$ for the following set of parameters: $U = 3$ eV, $V = 1$ eV, $J = 0.7$ eV, $J' = 0.3$ eV, $t_{11} = t_{22} = 1$ eV, and $t_{12} = t_{21} = 0.5$ eV. For example, for $\Delta = 1$ eV
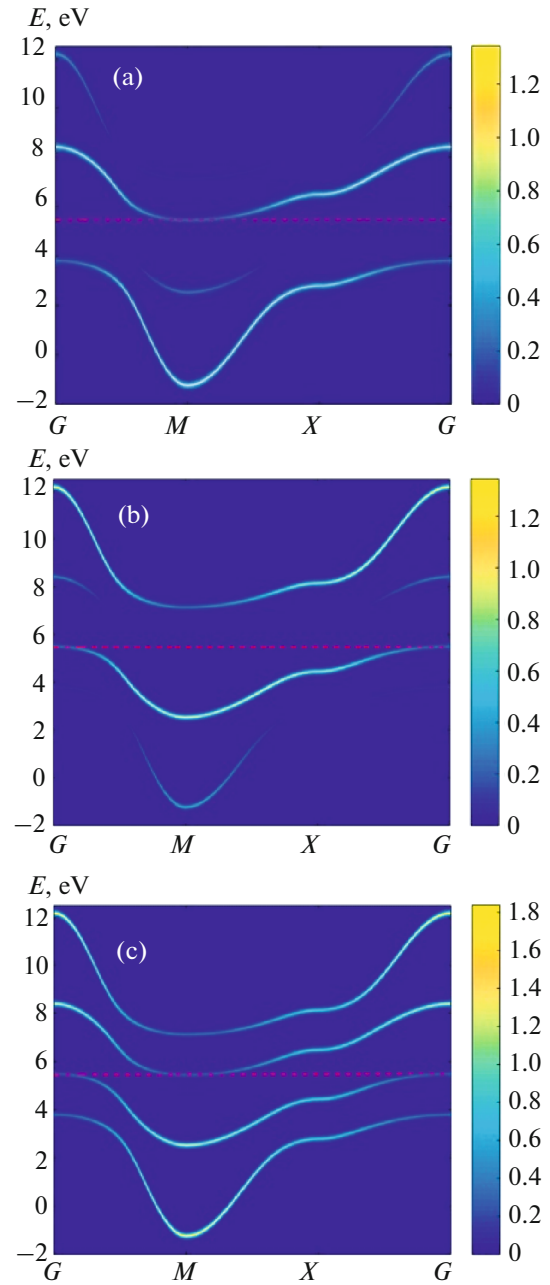
(see Fig. 2), the calculated band structure has an indirect dielectric gap E_g, and the Fermi energy lies in the bandgap. Here and below, the color represents the partial spectral weight distribution

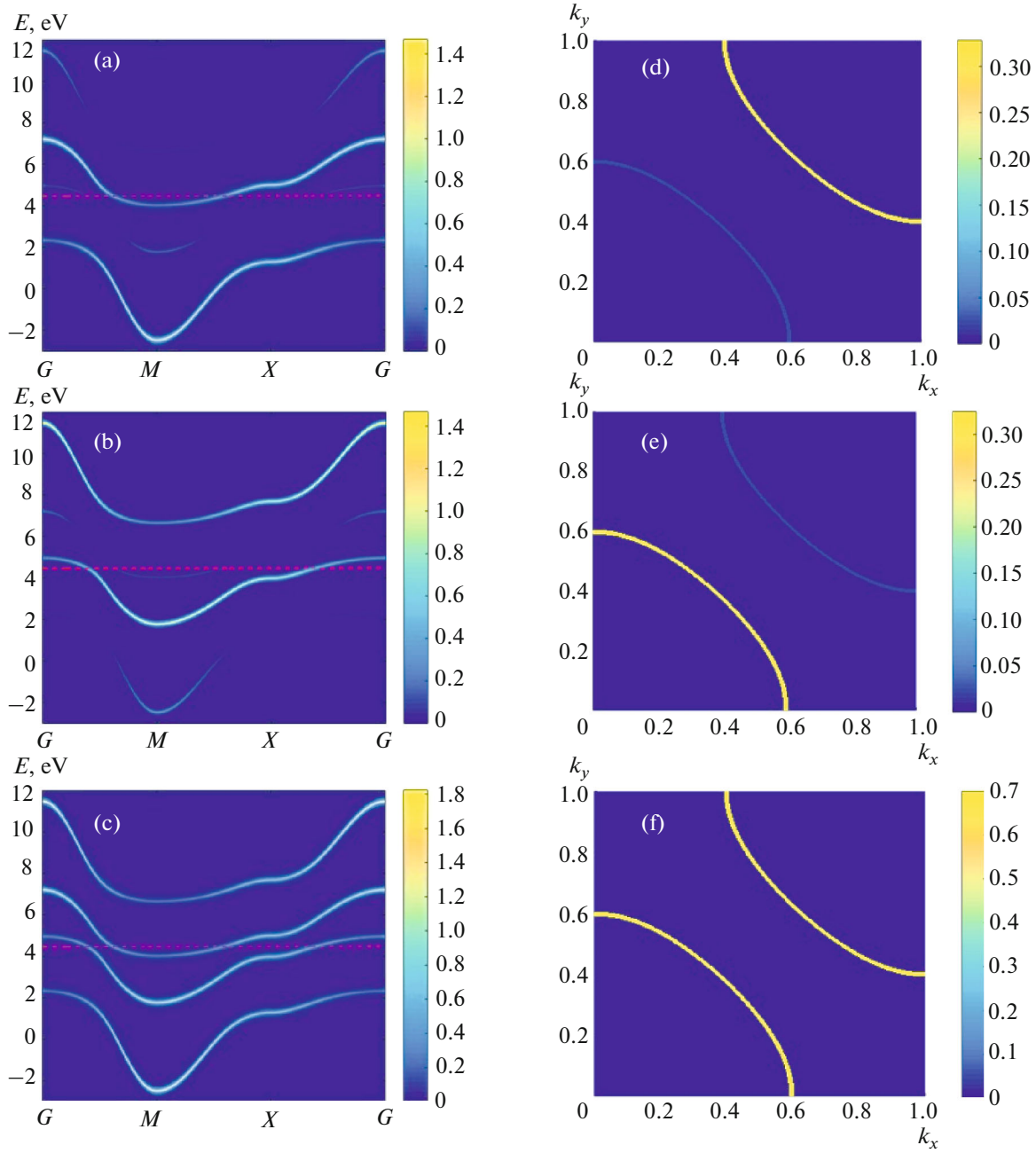$$A_\lambda(k, \omega) = \sum_\sigma A_{\lambda\sigma}(k, \omega)$$

Fig. 4. (Color online) Electronic structure calculated for the HS phase at $\Delta = \Delta_C - \delta$, $\delta \to 0$. Left column shows dispersion of Fermi quasiparticle excitations. Right column shows the corresponding Fermi surfaces. Colored curves show the distribution of the partial spectral weight of quasiparticle excitations in the first Brillouin zone for (a, d) $\lambda = 1$ (ε_1), (b, e) $\lambda = 2$ (ε_2), and (c, f) total spectral weight.

of Fermi quasiparticle excitations within the first Brillouin zone for $\lambda = 1$ (ε_1) (a), $\lambda = 2$ (ε_2) (b), and total spectral weight $A(k, \omega) = \sum_{\lambda,\sigma} A_{\lambda\sigma}(k, \omega)$ (c). Since the system in the HS phase is considered in the paramagnetic state and, accordingly, in the nonmagnetic state in the LS phase, we have $A_{\lambda\uparrow}(k, \omega) = A_{\lambda\downarrow}(k, \omega)$ everywhere. The horizontal red dashed line indicates the position of the Fermi level. For $\Delta \approx 1.64$ eV (see Fig. 3), the dielectric gap disappears ($E_g = 0$), and the Fermi surface of the hole and electron types opens at point $G(0, 0)$, $M(1, 1)$, respectively, of the first Brillouin zone. With increasing crystal field in the HS phase for $\Delta < \Delta_C$, the Fermi surface increases, and the overlapping of the valence band with the conduction band, which is typical of semimetals, is observed. Fig-
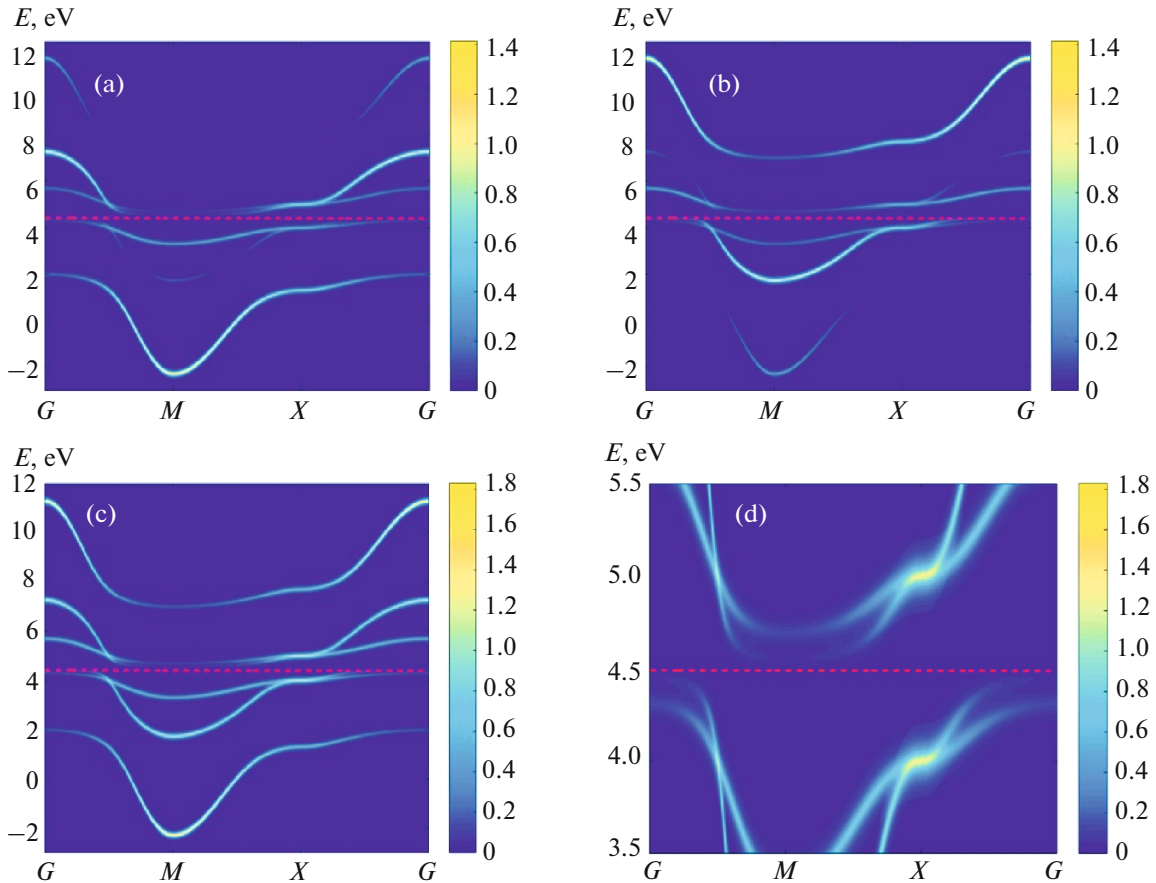
Fig. 5. (Color online) Electronic band structure calculated strictly at the crossover point for $\Delta = \Delta_C$, $\xi = 0$. Colored curves show the distribution of partial spectral weight of quasiparticle excitations in the first Brillouin zone for (a) $\lambda = 1$ (ε_1), (b) $\lambda = 2$ (ε_2), and (c, d) total spectral weight. The dispersion relation (c) is shown separately in (d) on a magnified scale near the Fermi level indicated by the horizontal red dashed line.

ure 4 shows the results of calculation of the electronic structure in the immediate vicinity of the crossover in the HS phase at $\Delta = \Delta_C - \delta$, $\delta \to 0$ (the value of δ was assumed to be 5×10^{-4} eV). However, exactly at the crossover point at $\Delta = \Delta_C$, a dielectric gap opens jumpwise in the electron spectrum (see Fig. 5). On the right of the crossover point in the LS phase for $\Delta = \Delta_C + \delta$, $\delta \to 0$, the system abruptly passes again to the semimetallic state (see Fig. 6) with the structure inverse relative to the initial band structure. Mutual inversion of the band can clearly be seen from comparison of the Fermi surfaces before and after the transition near Δ_C (see Figs. 4d, 4e and Figs. 6d, 6e). Here and below, the Fermi surface is shown for the first quarter of the first Brillouin zone. Therefore, in the absence of the spin–orbit interaction ($\xi = 0$), a sharp semimetal–insulator–semimetal transition typical of quantum phase transitions with band inversion occurs between the HS and LS states upon an increase in the crystal field near Δ_C.

Figure 7 shows for comparison the results of calculation of the Fermi surfaces in different phases of the HS and LS states in the vicinity of transition (upper and lower rows, respectively) with account for the distribution of the partial and total spectral weights, as well as the corresponding results of calculation of the surfaces of zeros of Green function $G_{\lambda\sigma}(k, \omega)$ and the total Green function

$$G_\sigma(k, \omega) = \sum_\lambda G_{\lambda\sigma}(k, \omega)$$

of quasiparticle excitations, which coincide for $\sigma = \pm 1/2$ (black color). Strictly at the crossover point ($\Delta = \Delta_C$), there is no Fermi surface. Apart from the evolution of surfaces themselves upon a change in the crystal field Δ near the crossover point, it can clearly be seen that close positions of poles and zeros of the Green function lead to a decrease in the spectral weight of the poles. The limiting case of their superposition corresponds to their annihilation. It can also be seen that a transition of the crystal field through the critical value leads to a sharp change in the topology of
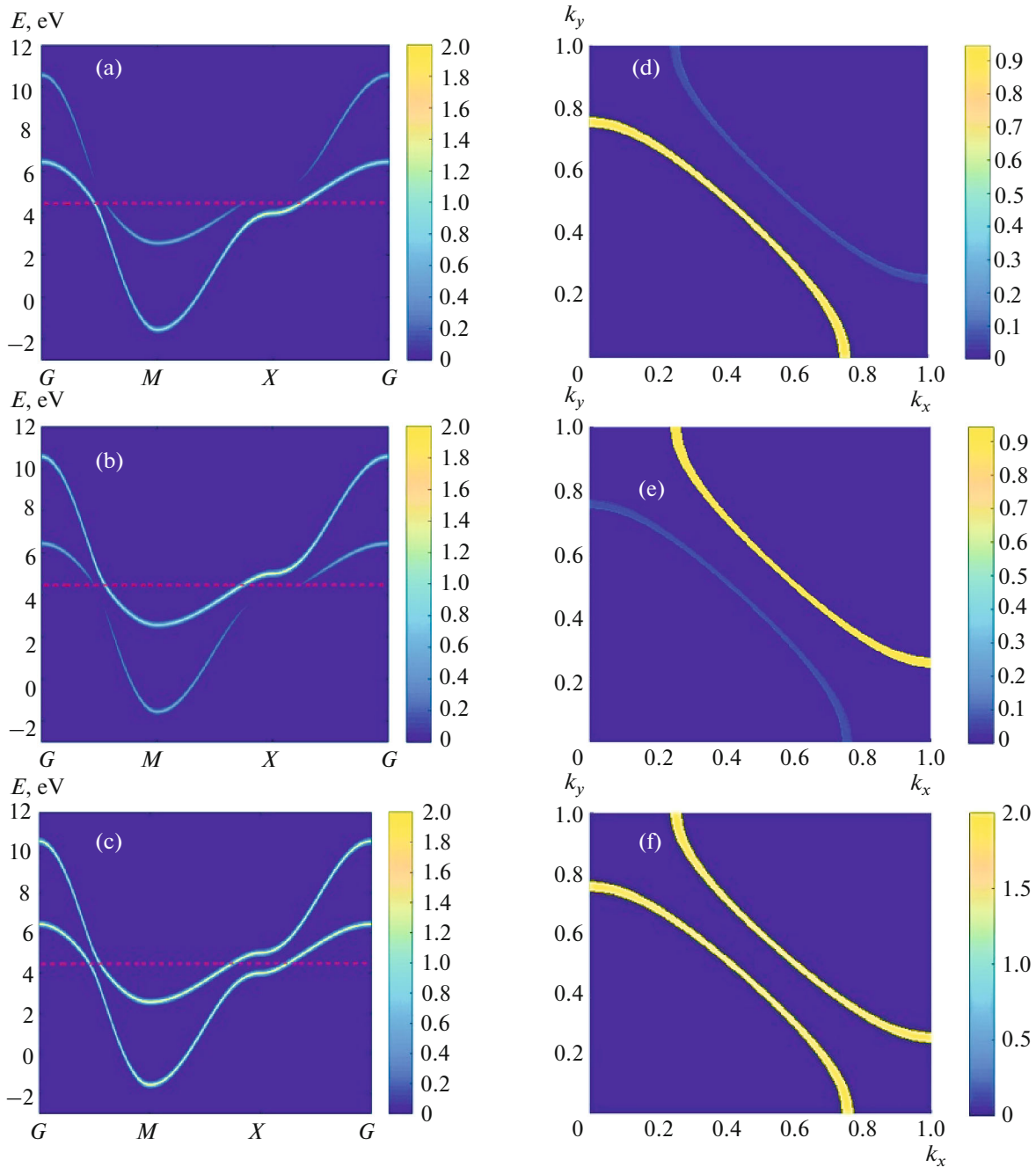
Fig. 6. (Color online) Electronic structure calculated for the LS phase at $\Delta = \Delta_C + \delta$, $\delta \to 0$. Left column shows dispersion of Fermi quasiparticle excitations. Right column shows the corresponding Fermi surface. Colored curves are the distributions of the partial spectral weight of quasiparticle excitations in the first Brillouin zone for (a, d) $\lambda = 1$ (ε_1); (b, e) $\lambda = 2$ (ε_2), and (c, f) total spectral weight.

the surfaces of Green function zeros, which considerably affects the redistribution of the partial spectral weight on the Fermi surface; however, the topology of the surfaces of the Green function poles does not change in this case. Therefore, the transition described above occurs with a change in the topological properties, which leads to the inversion of the band structure

and necessitates the opening of the dielectric gap at the transition point proper.

4. ROLE OF THE SPIN−ORBIT INTERACTION

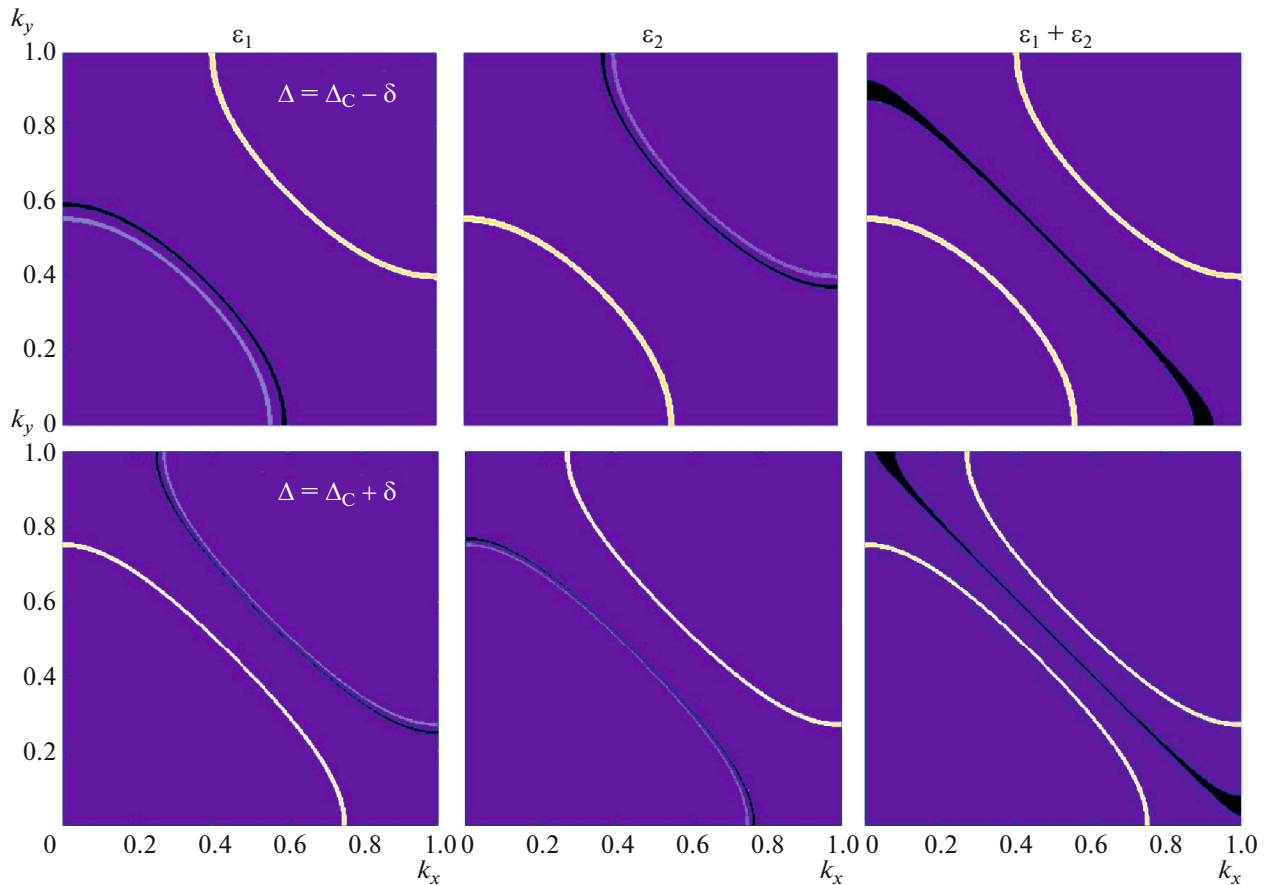In the presence of the spin−orbit interaction ξ, quantum-mechanical mixing of the HS and LS states

Fig. 7. (Color online) Fermi surface and the surface of zeros of the Green function for quasiparticles. Upper panel corresponds to the HS phase for $\Delta = \Delta_C - \delta$, $\delta = 5 \times 10^{-6}$ eV. Lower panel shows the phase of the LS state for $\Delta = \Delta_C + \delta$. Colored curves are the distributions of the partial spectral weight of quasiparticle excitations for $\lambda = 1$ (ε_1), $\lambda = 2$ (ε_2), and total spectral weight. The corresponding surfaces of Green function zeros for quasiparticles are shown by black curves.

takes place, and the ground state of the system becomes their linear combination [14]. Figure 8 shows the dependence of the energy of terms of the HS and LS states on crystal field Δ near Δ_C in the presence of the spin–orbit interaction with energy $\xi = 0.05$ eV between them (solid black curves). The red dashed line and the green dotted curve show for comparison the position of terms of the HS and LS states in the absence of the spin–orbit interaction ($\xi = 0$). The solid inclined black line coinciding with the dashed red line shows the Kramers doublet. Therefore, the quantum phase transition induced by the sharp change of the ground state of the system in the presence of the spin–orbit interaction is transformed into a smooth quantum crossover.

Figure 9 shows the results of calculation of the electronic band structure for $\Delta = \Delta_C$ with account for spin–orbit interaction $\xi = 0.05$ eV. The band structure is of the semimetal type. The splitting of the valence band and the conduction band induced by the spin–orbit interaction can be seen clearly. Since the ground

state of the system in this case is a superposition of the HS and LS states, the energy spectrum slightly on the left and on the right of Δ_C does not differ qualitatively in any way from the spectrum shown in Fig. 9. Therefore, the system can be continuously transferred through the crossover point without sharp singularities observed near Δ_C for $\xi = 0$. The dielectric ground state is unstable to the perturbation induced by the spin–orbit interaction.

In spite of the fact that in the presence of spin–orbit interaction ξ, the electronic band structure continuously changes during passage through the crossover point upon an increase in the crystal field, the topology of the surface of zeros of the total Green function $G_\sigma(k, \omega)$ still changes. Figure 10 shows for comparison the results of calculation of the Fermi surface and the surface of the full Green function zeros for quasiparticles in the absence ($\xi = 0$, left column) and in the presence ($\xi = 0.05$ eV, right column) of the spin–orbit interaction. Colored curves show the distribution of the total spectral weight $A(k, \omega)$ of quasi-
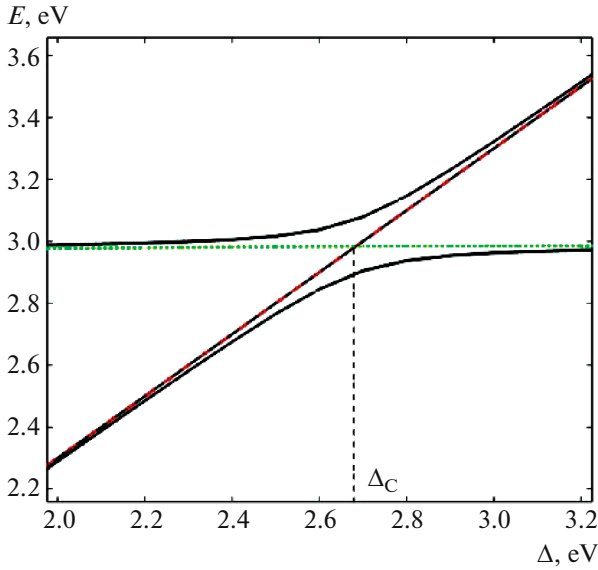
Fig. 8. (Color online) Dependences of the energy of terms of the HS and LS states on crystal field Δ near Δ_C in the presence of spin−orbit interaction $\xi = 0.05$ eV between them (solid black curves). Red dashed line and green dotted line show the positions of terms of the HS and LS states, respectively, in the absence of the spin−orbit interaction ($\xi = 0$).

particle excitations. The surfaces of zeros of full Green function $G_\sigma(k, \omega)$ of quasiparticles, which coincide for $\sigma = \pm 1/2$, are shown by black curves. Apart of the splitting associated with the spin−orbit interaction between the electron and hole parts of the Fermi surface and the surface of zeros, the change in the topology of the surface of zeros near Δ_C can be seen clearly. Therefore, even in the presence of the spin−orbit interaction leading to the quantum-mechanical mixing of the HS and LS states, the topological peculiarity in the shape variations of the surface of zeros of the full Green function for Fermi quasiparticle is preserved.

5. DISCUSSION AND CONCLUSIONS

Spin crossover at zero temperature is a quantum phase transition in pressure (crystal field growth) with the topological order parameter determined by the geometrical Berry phase, which changes abruptly by 2π at the transition point [4]. For this reason, it is interesting to trace the variation of the band structure during the spin crossover. In the framework of the two-band Hubbard model considered for a simple 2D square lattice, a semimetal−insulator−semimetal transition has been detected in the electron system with spin crossover upon an increase in the crystal field during the transition from the HS phase to the phase of the LS state. The abrupt opening of the dielectric gap in the electron excitation spectrum at the crossover point is associated with the band structure inversion, i.e., jumpwise redistribution of the par-

tial spectral weight of quasiparticle excitations between the electron and hole regions of the Fermi surface and a change in the topology of the surface of zeros of the Green function for quasiparticle excitations. It should be noted that simultaneous analysis of the surfaces of zeros and poles of the Green function at the Fermi level makes it possible to trace the topological changes in the electronic structure at the spin crossover point more accurately and reflects the essence of the method based on analysis of topological invariants [15].

We have considered the results of calculation of the electronic structure with account for the nondiagonal component of the spin−orbit interaction leading to the quantum-mechanical mixing of the HS and LS states and to a smooth variation of the ground state of the system upon an increase in the crystal field. It is shown that even in the presence of the spin−orbit interaction, a topological singularity was observed in the change of the shape of the surface of zeros of the full Green function for Fermi quasiparticle excitations. All calculations were performed for the paramagnetic HS state in the absence of magnetic ordering. However, in the presence of the cooperative superexchange interaction $\tilde{J}$, the system exhibits again a sharp change in the ground magnetically ordered HS (antiferromagnetic or ferromagnetic) state to the nonmagnetic LS state if $z\tilde{J} > \xi$, where z is the number of the nearest neighbors, but now for $\Delta > \Delta_C$ [16−19]. Therefore, despite the spin−orbit interaction, a sharp rearrangement of the electron spectrum occurs at the spin crossover point with a change in the topology of the Fermi surface and the surface of the Green function zeros. The calculation of the electronic band structure with allowance for the antiferromagnetic order is the subject of separate analysis.

Since the semimetallic HS and LS phases can be spatially separated, and their electronic band structures in the absence of the spin−orbit interaction cannot be transformed into each other continuously (without discontinuities), it can be proposed that the dielectric state can be formed at the interface between two phases analogously to the formation of the metal state at the interface between two dielectrics with a topologically nontrivial band structure. For this reason, concluding this section, we endeavor to consider in general the possibility of existence of a dielectric state at the interface between arbitrary semimetallic media with mutually inverted bands at the inverse contact on the basis of the model example of the correlated system with spin crossover given in this study. For this purpose, we recollect that topological electronic states were predicted by Volkov and Pankratov [20] as the boundary states at the inverse contact between semiconductors with mutually inverted bands (with opposite signs of the bandgap). This turned out to be a predecessor of a new quantum type of matter. Moreover, $Pb_{1-x}Sn_xTe_x$ semiconductor compounds
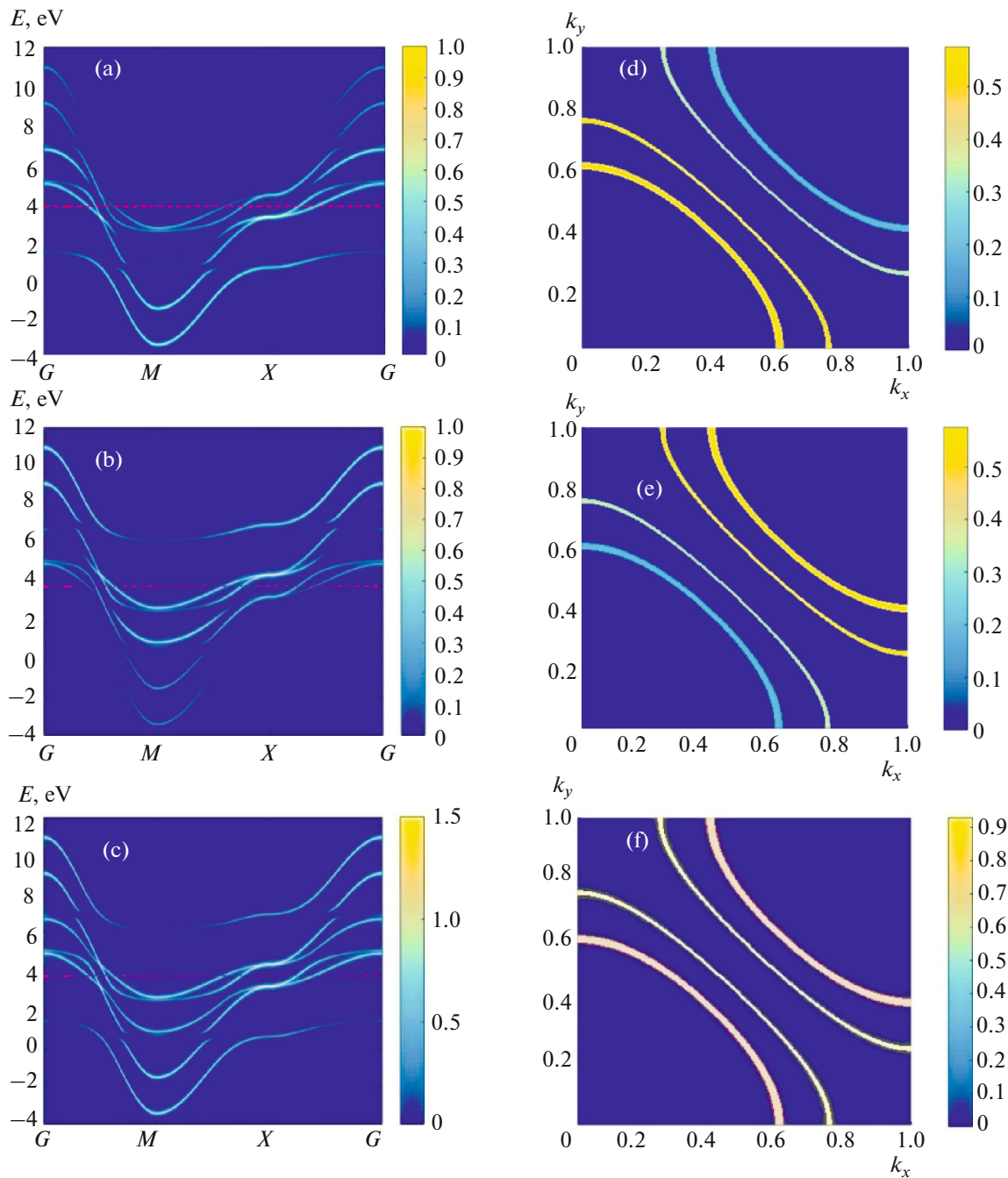
Fig. 9. (Color online) Electronic structure calculated strictly at the crossover point for $\Delta = \Delta_C$ in the presence of spin−orbit interaction $\xi = 0.05$ eV. Left column shows dispersion of Fermi quasiparticle excitations. Right column shows the corresponding Fermi surfaces. Colored curves are the distributions of the partial spectral weight of quasiparticle excitations for (a, d) $\lambda = 1$ (ε_1), (b, e) $\lambda = 2$ (ε_2), and (c, f) total spectral weight.

with band inversion, which were considered in [20] as the model system, in fact proved to be topological insulators [21]. It has become clear later that there is no need to synthesize an inverse contact to observe the Weyl states. The contact with vacuum, i.e., the existence of a surface, is sufficient. Since the SnTe "inverted" semiconductor is itself a topological insulator, the Weyl states always exist on its surface. Their topological stability is guaranteed by the crystal symmetry [22]. The model considered in [20] turned out to be the first example of a topological insulator, while the inverse contact served as an example of a topologically nontrivial interface [23]. Following [20], we propose the possibility of existence of a
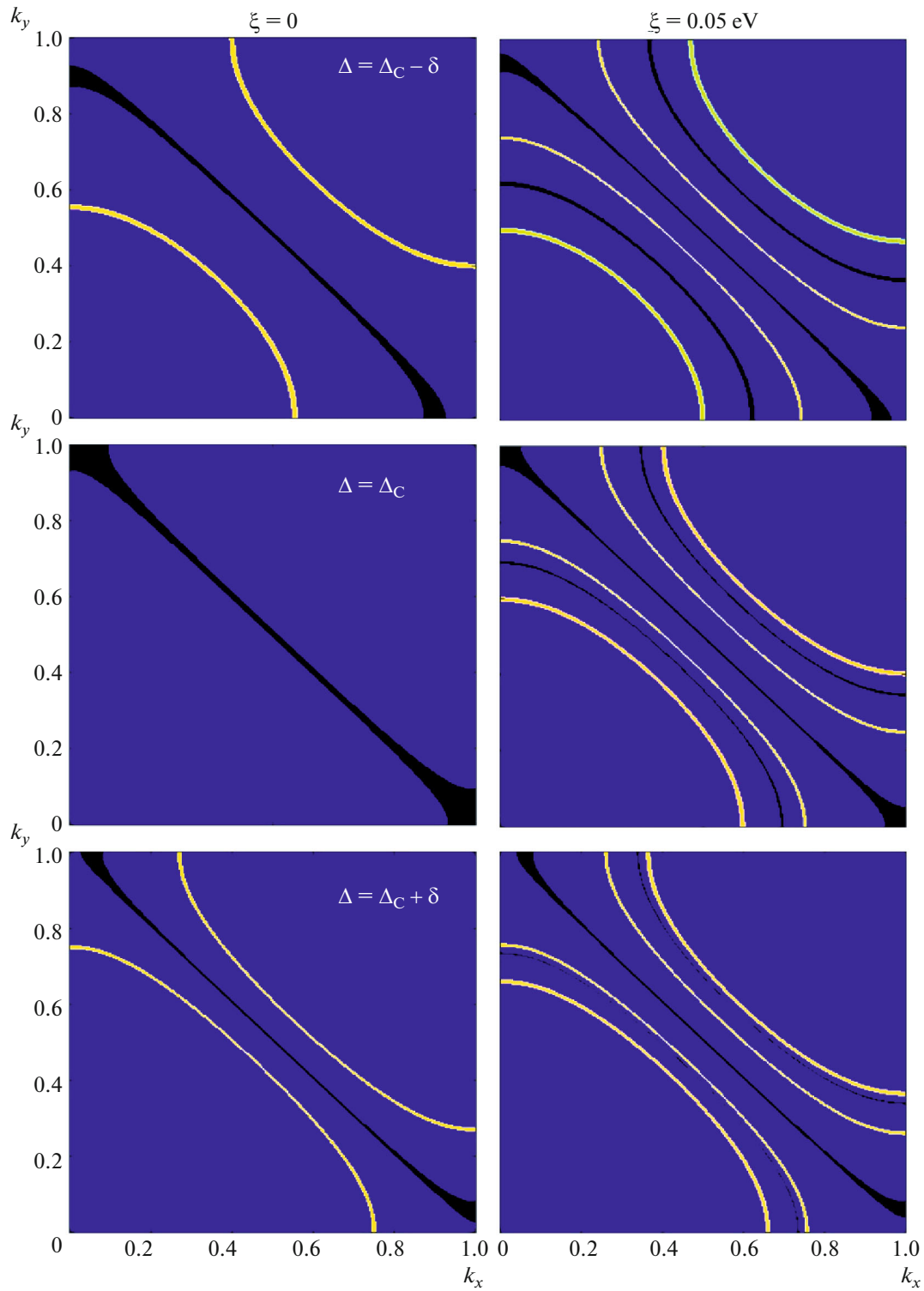
Fig. 10. (Color online) Fermi surface and the surface of Green function zeros for quasiparticles. Upper panel corresponds to the HS phase for $\Delta = \Delta_C - \delta$, $\delta = 5 \times 10^{-6}$ eV. Lower panel shows the phase of the LS state for $\Delta = \Delta_C + \delta$. Middle panel corresponds to $\Delta = \Delta_C$. Colored curves are the distributions of the total spectral weight of quasiparticle excitations in the absence of the spin–orbit interaction ($\xi = 0$) and in the presence of the spin–orbit interaction ($\xi = 0.05$). The corresponding surface of zeros of Green function $G_\sigma(k, \omega)$ of quasiparticles, which coincide for $\sigma = \pm 1/2$, are shown by black curves.

dielectric surface state in heterostructures based on semimetals with an inversion of the electronic band structure similar to that described in this article in contrast to the existence of a metal state at the interface between two dielectrics with a topologically nontrivial band structure.

REFERENCES

1. F. Renz, J. Phys.: Conf. Ser. **217**, 012022 (2010).
2. *Spin Crossover in Transition Metal Compounds I–III*, Ed. by P. Gütlich and H. A. Goodwin (Springer, Berlin, 2004).
3. *Spin-Crossover Materials: Properties and Applications*, Ed. by M. A. Halcrow (Wiley, Oxford, UK, 2013).
4. A. I. Nesterov and S. G. Ovchinnikov, JETP Lett. **90**, 530 (2009).
5. K. I. Kugel' and D. I. Khomskii, Sov. Phys. JETP **37**, 725 (1973).
6. K. I. Kugel' and D. I. Khomskii, Sov. Phys. Usp. **25**, 231 (1982).
7. S. V. Streltsov and D. I. Khomskii, Phys. Usp. **60**, 1121 (2017).
8. J. Kuneš, J. Phys.: Condens. Matter **27**, 333201 (2015).
9. W. Brzezicki, J. Dziarmaga, and A. M. Oles, Phys. Rev. Lett. **109**, 237201 (2012).
10. L. V. Keldysh and Yu. V. Kopaev, Sov. Phys. Solid State **6**, 2219 (1964).
11. M. Haverkort, Ph. D. Thesis (Univ. Köln, 2005).
12. R. O. Zaitsev, Sov. Phys. JETP **43**, 5574 (1976).
13. S. G. Ovchinnikov and V. V. Val'kov, *Hubbard Operators in the Theory of Strongly Correlated Electrons* (Imperial College Press, London, Singapore, 2004).
14. J. S. Griffith, *The Theory of Transition-Metal Ions* (Cambridge Univ. Press, Cambridge, 1961).
15. G. E. Volovik, *The Universe in a Helium Droplet* (Oxford Univ. Press, New York, 2003).
16. Yu. S. Orlov, S. V. Nikolaev, A. I. Nesterov, and S. G. Ovchinnikov, JETP Lett. **105**, 771 (2017).
17. A. I. Nesterov, Yu. S. Orlov, S. V. Nikolaev, and S. G. Ovchinnikov, Phys. Rev. B **96**, 134103 (2017).
18. Yu. S. Orlov, S. V. Nikolaev, and S. G. Ovchinnikov, J. Exp. Theor. Phys. **129**, 1062 (2019)].
19. V. I. Kuz'min, Yu. S. Orlov, A. E. Zarubin, T. M. Ovchinnikova, and S. G. Ovchinnikov, Phys. Rev. B **100**, 144429 (2019).
20. B. A. Volkov and O. A. Pankratov, JETP Lett. **42**, 178 (1985).
21. Y. Tanaka, Zhi Ren, T. Sato, K. Nakayama, S. Souma, T. Takahashio, K. Segawa, and Y. Ando, Nat. Phys. **8**, 800 (2012).
22. T. H. Hsieh, H. Lin, J. Liu, W. Duan, A. Bansil, and L. Fu, Nat. Commun. **3**, 982 (2012).
23. O. A. Pankratov, Phys. Usp. **61**, 1116 (2018).

Translated by N. Wadhwa